Nucleon form factors and final state radiative corrections to $e^+e^- \to \bar{p}p\gamma^*$

Henryk Czyż,[1] Johann H. Kühn,[2] and Szymon Tracz[1]

[1] *Institute of Physics, University of Silesia, PL-40007 Katowice, Poland.*
[2] *Institut für Theoretische Teilchenphysik, Karlsruhe Institute of Technology, D-76128 Karlsruhe, Germany.*

(Dated: November 21, 2014)

New parametrisation for the electric and the magnetic form factors of proton and neutron are presented. The proton form factors describe well the recent measurements by BaBar collaboration and earlier ones of the ratio of the form factors in space-like region. The neutron form factors are consistent with earlier measurements of neutron pair production and ratio of the form factors in the space-like region. These form factors are implemented into the generator PHOKHARA, which simulates the reactions $e^+e^- \to \bar{p}p\gamma$ and $e^+e^- \to \bar{n}n\gamma$. The influence of final state radiation is investigated.

PACS numbers: 13.66.Bc, 13.40.Gp

arXiv:1407.7995v2 [hep-ph] 19 Nov 2014

I. INTRODUCTION

Nucleon form factors both in the space-like and in the time-like regions have attracted theoretical as well as experimental attention from the early times of particle physics [1–4]. Experiments for electron-proton scattering give access to the space-like region and detailed analyses of angular distributions without [2] and with [5] polarised beam and target allow to separate the magnetic and electric form factors. The cross section for proton-antiproton production at electron-positron colliders (or the inverse reaction $p\bar{p} \to e^+e^-$) gives access to a specific combination of form factors in the time-like region. The additional analysis of angular distributions allows to separate magnetic and electric form factors. Recently discrepancies have been found between the ratio of magnetic and electric form factors extracted in the space-like region using the Rosenbluth method or, alternatively, using polarised beam and/or target (see [6] for a review). The mentioned inconsistency was to large extent explained theoretically by enhanced contributions from two photon exchange (see [7] for a review). Nevertheless this has triggered a new experiment (OLYMPUS) [8] to measure both electron and positron scattering off protons and designed to resolve this issue experimentally. Form factors in the space- and time-like regions are connected via analyticity. Thus measurements in e^+e^- collisions may help to resolve this issue. Even more important, these measurements are ideally suited to search for baryon-antibaryon resonances close to production threshold as well as at higher energies. Last but not least, the high energy behaviour has been predicted in the frame work of perturbative QCD [9], predictions that could be checked at high energy. For recent reviews on nucleon electromagnetic form factors we refer the reader to [10] and [11].

There are three reactions that are currently used for measurements in the time-like region: $e^+e^- \to p\bar{p}$, $p\bar{p} \to e^+e^-$ and the radiative return reaction $e^+e^- \to p\bar{p}\gamma$. Given sufficiently large luminosity, the third reaction allows to measure the form factors in principle from threshold up to the collider energy. The radiative return has been employed successfully by the BaBar experiment [12], which has measured the production rate and the ratio of the form factors with a precision of 7% and 11% respectively. In view of this improvement we present a parametrisation of the nucleon form factors, which is based on generalised vector dominance, similar to that from [13] for the case of pion and kaon pair production. Furthermore we consider in detail the impact of final state radiation to this measurement. In our simplified model we treat real radiation similar to the radiation from a point-like particle. As far as the virtual corrections are concerned we include the Coulomb enhancement factor, important close to threshold and an infrared subtraction term to compensate for soft real radiation. These ingredients are implemented into Monte Carlo event generator PHOKHARA, version 9.1 and the effect of these modifications is studied in detail. Additionally, the same modifications are added to the description of proton-antiproton pair production in the scanning mode ($e^+e^- \to p\bar{p}$) in PHOKHARA version 9.1.

II. NUCLEON FORM FACTORS

In the first implementation [14] of nucleon pair production through the radiative return ($e^+e^- \to \bar{N}N\gamma$) into the event generator PHOKHARA a model of the nucleon form factors was used, which had been taken from [15]. To accommodate the experimental data, which are available now, we propose a new, improved model for the Dirac and Pauli nucleon form factors

$$F^p_{1,2} = F^s_{1,2} + F^v_{1,2}, \quad (1)$$

$$F^n_{1,2} = F^s_{1,2} - F^v_{1,2}, \quad (2)$$

*Work supported in part by the Polish National Science Centre, grant number DEC-2012/07/B/ST2/03867 and German Research Foundation DFG under Contract No. Collaborative Research Center CRC-1044.

which enter the electromagnetic current

$$J_\mu = -ie\bar{v}(p_2)\left(F_1^N(Q^2)\gamma_\mu - \frac{F_2^N(Q^2)}{4m_N}[\gamma_\mu, \not{Q}]\right)u(p_1); \tag{3}$$

where $Q = p_1 + p_2$. The indices s and v refer to isospin zero and one respectively.

We use the following ansatz

$$F_1^s = \frac{1}{2}\frac{\sum_{n=0}^4 c_n^1 BW_{\omega_n}(s)}{\sum_{n=0}^4 c_n^1}, \tag{4}$$

$$F_1^v = \frac{1}{2}\frac{\sum_{n=0}^4 c_n^2 BW_{\rho_n}(s)}{\sum_{n=0}^4 c_n^2}, \tag{5}$$

$$F_2^s = -\frac{1}{2}b\frac{\sum_{n=0}^4 c_n^3 BW_{\omega_n}(s)}{\sum_{n=0}^4 c_n^3}, \tag{6}$$

$$F_2^v = \frac{1}{2}a\frac{\sum_{n=0}^4 c_n^4 BW_{\rho_n}(s)}{\sum_{n=0}^4 c_n^4}, \tag{7}$$

where $c_0^i = 1$ for $i = 1, 2, 3, 4$. Following the Zweig rule we neglect the ϕ contributions. The Breit - Wigner function is defined as:

$$BW_i(Q^2) = \frac{m_i^2}{m_i^2 - Q^2 - im_i\Gamma_i\theta(Q^2)}. \tag{8}$$

The step function $\theta(Q^2)$ sets the mesons widths to zero for space-like Q^2. Above the proton-anti-proton production threshold we use constant meson widths. The normalisation of electric and magnetic form factors in the limit of $s = 0$ to electric charges and magnetic moments of nucleons fixes the parameters $a = \mu_p - \mu_n - 1$ and $b = -\mu_p - \mu_n + 1$, where $\mu_p(\mu_n)$ are the magnetic moments of proton (neutron). We impose the asymptotic (large Q^2) behaviour of the form factors predicted in perturbative QCD [9]

$$F_1 \sim \frac{1}{(Q^2)^2}, \qquad F_2 \sim \frac{1}{(Q^2)^3}, \tag{9}$$

which leaves six independent complex parameters to be determined by experimental data. Below we rewrite them using real parameters $c_i^j = c_i^{jR} + ic_i^{jI}\theta(Q^2)$.

The asymptotic behaviour, Eq.(9), is enforced by choosing

$$c_4^1 = -\frac{1}{m_{\omega_4}^2}\sum_{n=0}^3 m_{\omega_n}^2 c_n^1 \tag{10}$$

$$c_4^2 = -\frac{1}{m_{\rho_4}^2}\sum_{n=0}^3 m_{\rho_n}^2 c_n^2 \tag{11}$$

$$c_3^3 = \frac{\sum_{n=0}^2 m_{\omega_n}^2 c_n^3 (m_{\omega_n}^2 - m_{\omega_4}^2 + i(m_{\omega_4}\Gamma_{\omega_4} - m_{\omega_n}\Gamma_{\omega_n}))}{m_{\omega_3}^2(m_{\omega_4}^2 - m_{\omega_3}^2 + i(m_{\omega_3}\Gamma_{\omega_3} - m_{\omega_4}\Gamma_{\omega_4}))},$$

$$c_4^3 = -\frac{1}{m_{\omega_4}^2}\sum_{n=0}^3 m_{\omega_n}^2 c_n^3 \tag{12}$$

$$c_3^4 = \frac{\sum_{n=0}^2 m_{\rho_n}^2 c_n^4 (m_{\rho_n}^2 - m_{\rho_4}^2 + i(m_{\rho_4}\Gamma_{\rho_4} - m_{\rho_n}\Gamma_{\rho_n}))}{m_{\rho_3}^2(m_{\rho_4}^2 - m_{\rho_3}^2 + i(m_{\rho_3}\Gamma_{\rho_3} - m_{\rho_4}\Gamma_{\rho_4}))},$$

$$c_4^4 = -\frac{1}{m_{\rho_4}^2}\sum_{n=0}^3 m_{\rho_n}^2 c_n^4. \tag{13}$$

$$\tag{14}$$

The Dirac and Pauli form factors for each nucleon N are related to the electric G_E^N and magnetic G_M^N through ($\tau = Q^2/4m_N^2$)

$$G_E^N = F_1^N + \tau F_2^N, \tag{15}$$

$$G_M^N = F_1^N + F_2^N. \tag{16}$$

Experiment	nep	χ^2	Experiment	nep	χ^2
BaBar cs [12]	38	30	BaBar r [12]	6	0.6
$PS170_1$ cs [16]	8	109	PS170 r [16]	5	16
$PS170_2$ cs [17]	4	4	$PS170_3$ cs [18]	4	52
$E760_1$ cs [19]	3	0.5	$E835_1$ cs [20]	5	1
$E835_2$ cs [21]	2	0.03	DM2 cs [22, 23]	7	26
BES cs [24]	8	10	CLEO cs [25]	1	0.4
FENICE cs [26]	5	5	DM1 cs [27]	4	0.7
JLab 05 r [28]	10	16	JLab 02 r [29]	4	1
JLab 01 r [30]	13	10	JLab 10 r [31]	3	6
MAMI 01 r [32]	3	2	JLab 03 r [33]	3	6
BLAST 08 r [34]	4	6	FENICE cs [26]	4	0.6
			SLAC cs [35]	32	27

TABLE I: *Values of the chi-squared distribution for particular experiments; nep- number of experimental points; cs - cross section; r- ratio of the electric and magnetic form factors. The PS170 and DM2 data were excluded from this fit - see text for details.*

c_1^{1R}	-0.45(1)	c_1^{1I}	-0.54(2)	c_2^{1R}	-0.27(1)	c_2^{1I}	0.18(1)
c_3^{1R}	0.42(2)	c_3^{1I}	0.37(2)	c_1^{2R}	-0.12(1)	c_1^{2I}	-3.06(2)
c_2^{2R}	0.16(1)	c_2^{2I}	2.53(1)	c_3^{2R}	-0.32(1)	c_3^{2I}	-0.17(1)
c_1^{3R}	-8.03(5)	c_1^{3I}	3.28(2)	c_2^{3R}	10.6(1)	c_2^{3I}	0.2(3)
c_1^{4R}	-0.845(1)	c_1^{4I}	0.364(1)	c_2^{4R}	0.427(1)	c_2^{4I}	-0.305(1)

TABLE II: *Parameters of the nucleons form factor for the fit, where the PS170 and DM2 data were excluded- see text for details.*

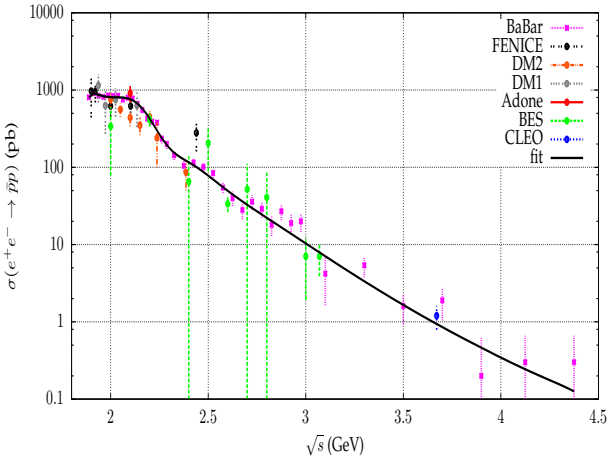

FIG. 1: (color online) The experimental data compared to the model fits results.

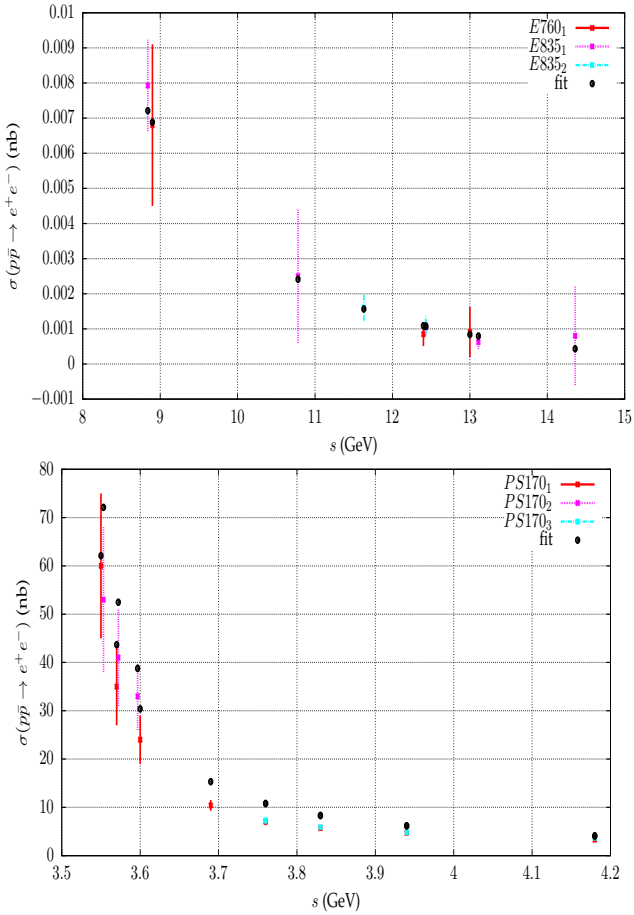

FIG. 2: (color online) The experimental data compared to the model fits results.

The masses and widths of the mesons and nucleons were taken from PDG [36] with the exception of $\rho_{3,4}$ and $\omega_{3,4}$ adopted from kaon form factor model [13] (m_{ρ_3} = 2.12 GeV, Γ_{ρ_3} = 0.3 GeV, m_{ω_3} = 2.0707 GeV, Γ_{ω_3} = 1.03535 GeV, m_{ρ_4} = 2.32647 GeV, Γ_{ρ_4} = 0.4473 GeV, m_{ω_4} = 2.34795 GeV, Γ_{ω_4} = 1.173975 GeV). The model parameters, namely the complex $V\bar{N}N$ couplings, were fitted to the following experimental data: $e^+e^- \to \bar{p}p$ cross section [12, 22–27, 37], $\bar{p}p \to e^+e^-$ cross section [16–21], $e^+e^- \to \bar{n}n$ cross section [26], ratio of the proton electric and magnetic form factors in the space-like [28–31] and the time-like [12, 16] regions and ratio of the neutron electric and magnetic form factors in the space-like region [33, 34]. The cross sections of the reaction $ep \to ep$, which depend also on the form factors we model, contain also non-negligible contributions from two-photon exchange diagrams [7]. The modelling of these contributions is beyond the scope of this paper and we adopted the following procedure to get a reasonable description of this cross section as well: We consider only one data set [35] covering large range of angles and kinematical invariant (Q^2). In fit we neglect the contribution from two-photon exchange diagrams and to account for this we enlarge the cross section error bars used in the fitting procedure to 10 % of the cross section.

A fit to all the above experimental data leads to unacceptable results (χ^2 = 214 for 177 data points). The reason is that the PS170 [16–18] and DM2 [22, 23]) data are in conflict with the BaBar data [12]. It is quite implausible that any model can accommodate PS170 and BaBar data sets at the same time as the ratio of the form factors is in evident conflict and, even more important, both $e^+e^- \to \bar{p}p$ and $\bar{p}p \to e^+e^-$ cross sections are proportional to the same combination of the magnetic and electric form factors $\left(|G_M^p|^2(1+\cos^2\theta) + \frac{|G_E^p|^2}{\tau}\sin^2\theta\right)$ (where θ is the scattering angle) and thus the same function is measured in both cases.

The model accommodates well the whole data set if one excludes either PS170 and DM2 (χ^2 = 124 for 150 data points) or BaBar data (χ^2 = 107 for 133 data points). In both cases the χ^2 values are excellent, but each of the models is in strong conflict with the data set which was not fitted. We report here only the details of the fit (Tables I and II, Figs. 1-4), were PS170 and DM2 data were excluded. Nevertheless it would be highly desirable to confirm the BaBar data by an independent measurement with similar precision. One observes (Fig. 4) that for model building a more accurate neutron-anti-neutron cross section would be desirable as the presently available data give little constraints on the model parameters.

III. FSR CORRECTIONS TO $e^+e^- \to \bar{p}p\gamma$

The BaBar data set was obtained with the radiative return method, and final state photon(s) emission was argued to be negligible [12]. As an independent data set might be obtained for example via radiative return method with higher accuracy the role of final state emis-

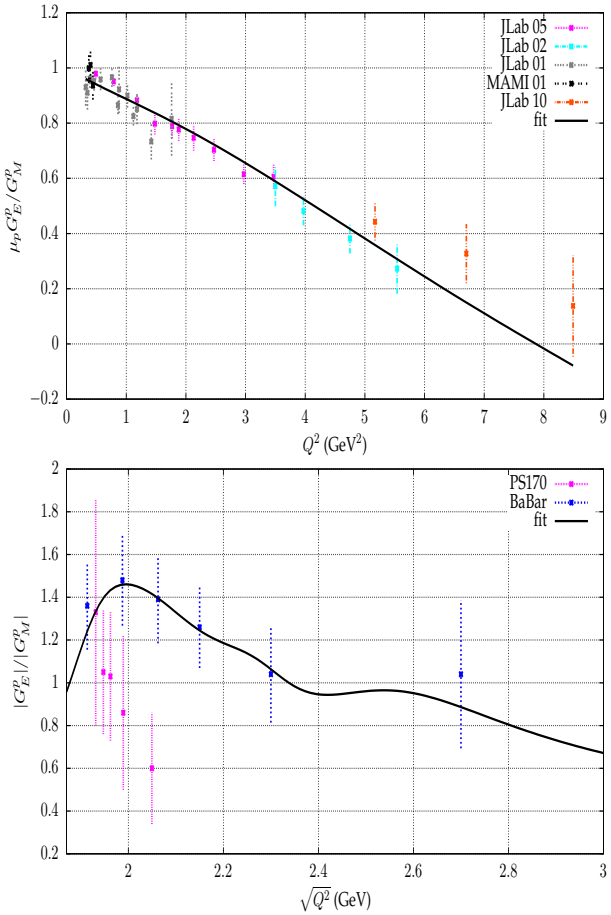

FIG. 3: (color online) The experimental data compared to the model fits results. Ratio of the electric and magnetic proton form factors in space-like (upper plot) and time-like (lower plot) regions.

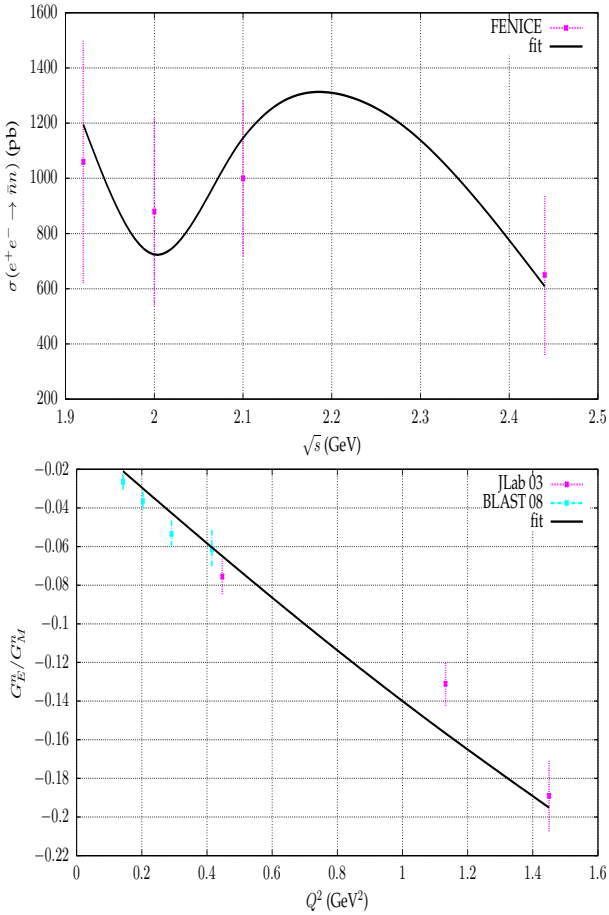

FIG. 4: (color online) The experimental data compared to the model fits results. Neutron-antineutron production cross section (upper plot) and ratio of the electric and magnetic neutron form factors in space-like region (lower plot).

sion has to be reconsidered. As evident from the previous section photon-nucleon interactions are not well known. Modelling of real photon emission from a proton is thus difficult. We follow here the scheme adopted successfully in [38] for final state emission from charged pions. For the proton the situation is more complicated, as due to the presence of the Pauli form factor at LO, the model is not normalisable. Here we adopted the simplest model assuming that real photon emission from a proton (anti-proton) looks like emission from a point-like charged particle. This means that it is identical to the emission from muons [39]. For the virtual corrections one cannot simply adapt the corrections from the muon case. Due to the presence of the F_2 form factor they are not the same and the corrections proportional to F_1 and F_2 are not expected to be identical. Moreover as the theory based on the interaction Lagrangian $\mathcal{L} = A^\mu J_\mu$ with A_μ being the electromagnetic field and J_μ defined in Eq.(3), is not renormalisable, further complications arise. They will not be addressed in this paper. For the virtual corrections we have used an overall factor, multiplying zero-, one- and two-photon emission parts:

$$C(Q^2) = f(\pi\alpha/\beta) - f(\pi\alpha) + 1, \tag{17}$$

where

$$f(x) = \frac{x}{1-\exp(-x)}\,, \qquad \beta = \sqrt{1-4m_p^2/Q^2}\,, \tag{18}$$

m_p is the proton mass and Q^2 is the invariant mass of proton-anti-proton pair.

At small proton velocities $C(Q^2)$ reproduces the usual Coulomb factor which resumes the leading radiative corrections for small velocities, while at large invariant masses $C(Q^2 \to \infty) \to 1$. In addition a correction of the form

$$\Delta_{final} = \frac{2\alpha}{\pi}\left[\frac{(1+\beta^2)}{2\beta}\log\frac{Q^2(1+\beta)^2}{4m_p^2} - 1\right]\log 2w \tag{19}$$

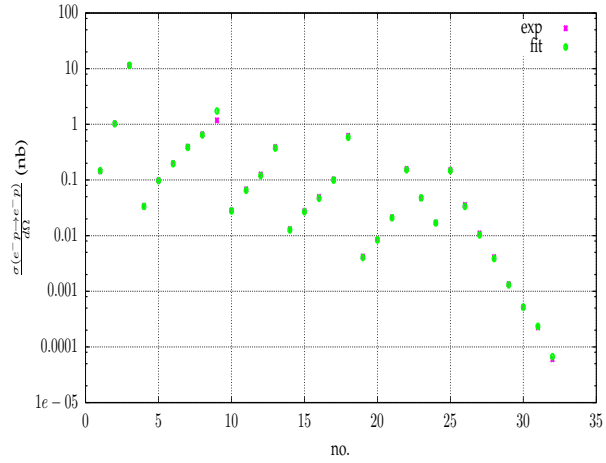

FIG. 5: (color online) The experimental data [35] compared to the model fit results. The data points and fit results are overlaid for most cases. On the horizontal axis the entry number from Table IV of [35] is given.

with $w = E_{\gamma,min}/\sqrt{s}$ was added , where $E_{\gamma,min}$ is a separation parameter between soft and hard parts of the photon phase space. It compensates the divergences arising from integration of a real emitted photon with energy $E_\gamma > E_{\gamma,min}$. Technically it leads to the replacement of $\frac{\alpha}{\pi}\eta^{V+S}$ used for muons in [39] with Δ_{final}. The factor C takes care of the proper threshold behaviour. Both C and Δ_{final} factors are generic for any model, which assumes that for soft photon emission proton behaves like a point-like particle. In any more elaborated model for the virtual corrections there will be additional finite corrections proportional to α/π, which will depend on the model details. In our ansatz we put them to zero. They are not expected to be big and their size can be tested using charge asymmetries as proposed in [38, 40, 41] for pion pair production. In our opinion without experimental tests of the FSR corrections better modelling of these contributions is not possible.

The size of FSR radiative corrections depends both on energy of an experiment and on the event selection used and can be both negative or positive. In Fig. 6 we show its size for an event selection close to the one used by BaBar. We show there a relative difference of the ISR cross section calculated at NLO and the ISR cross section corrected with with Coulomb factor

$$C_F(Q^2) = f(\pi\alpha/\beta). \tag{20}$$

The difference between the FSR correction calculated with Coulomb factor only and FSR at NLO is also shown in Fig. 6. Its typical size is of order one percent. In Fig. 7 we show the same differences calculated at a possible BES-III energy. The FSR corrections not included in the Coulomb factor $C_F(Q^2)$ are here even lower then at BaBar energy, but still of order of one percent at low proton-anti-proton pair invariant masses. As the FSR corrections for proton antiproton pair production were

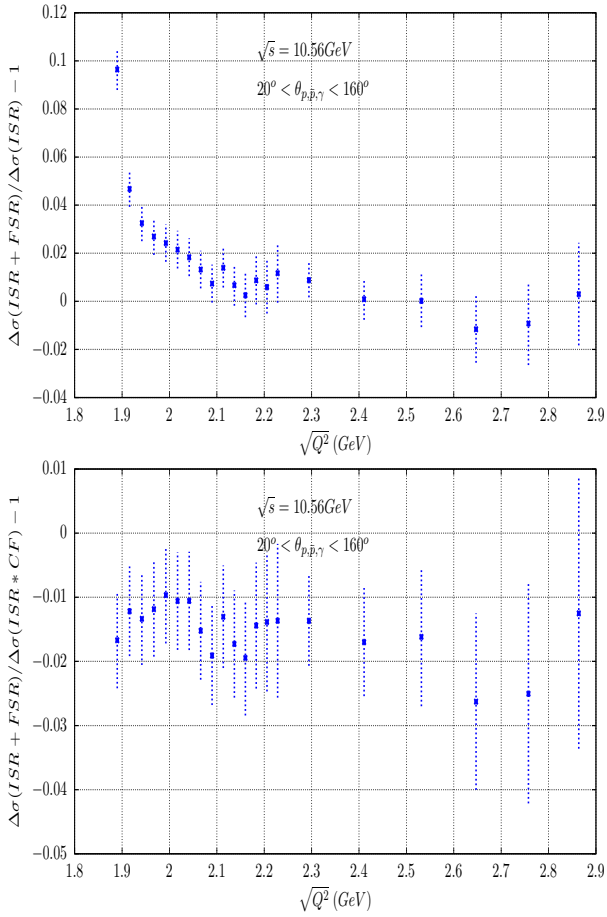

FIG. 6: (color online) Relative difference between Q^2 distributions calculated at NLO with and without FSR radiative corrections and between complete FSR corrections and FSR corrections where only Coulomb factor is included.

not tested experimentally the one percent contribution coming from our model should be taken conservatively as an estimate of the accuracy of the modelling of the FSR.

FSR corrections were also implemented for proton antiproton final state in the 'scan' mode of the PHOKHARA Monte Carlo event generator [42]. Only the Coulomb factor Eq. (20) was taken into account. Its size is demonstrated in Fig. 8. From this figure one can see that in any scan experiment in the region close to the threshold where in principle one can test the resummation of radiative corrections the beam energy smearing effects (where beam spread is typically 1-2 MeV) will obscure the effect. The distance between the first two points is taken as 1.5 MeV while between the second and the third point the step size is 2 MeV.

The event generator PHOKHARA 9.1, which includes the new nucleon form factors and final state corrections is available at the web page `http://ific.uv.es/~rodrigo/phokhara/` . The newly added part of the code proportional to the Pauli form factor with real photon emission was tested using

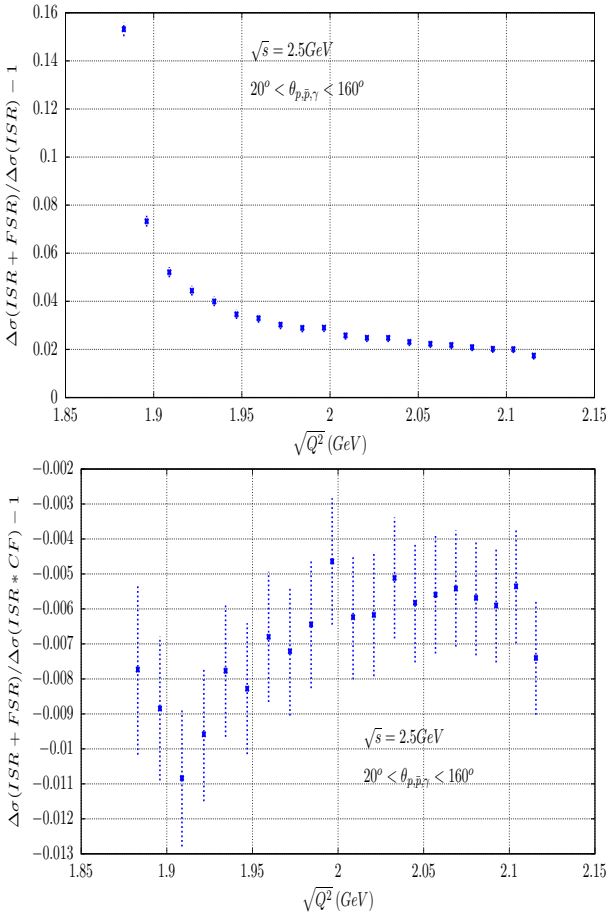

FIG. 7: (color online) Relative difference between Q^2 distributions calculated at NLO with and without FSR radiative corrections and between complete FSR corrections and FSR corrections where only Coulomb factor is included.

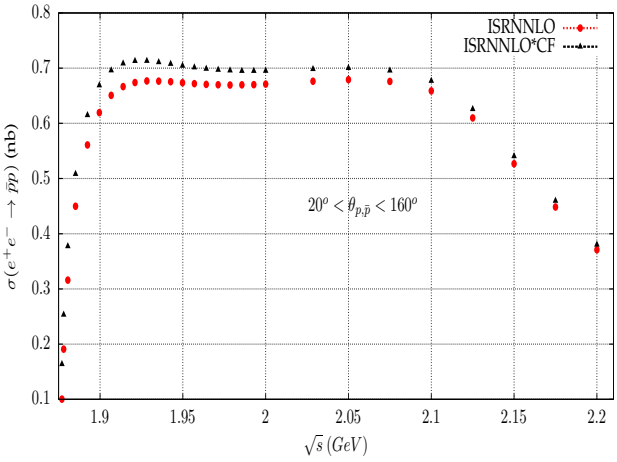

FIG. 8: (color online) The cross section of the reaction $e^+e^- \to \bar{p}p$ with ISR at NNLO corrections included is compared to the same cross section where in addition FSR Coulomb corrections were added.

an independently written code. In the distributed code the helicity amplitude method is used. Tests on independence of the cross section on the soft-hard photon separation parameter w were also performed with the accuracy not worse than 0.03%.

IV. CONCLUSIONS

We have constructed nucleon form factors on the basis of generalised vector dominance which are consistent with recent BaBar results for proton-antiproton production through the radiative return, with older data for neutron-antineutron production and with results for electron-nucleon scattering. Furthermore these form factors exhibit the the high energy behaviour predicted from perturbative QCD. We have considered the effect of final state radiation, demonstrating its smallness for typical experimental cuts. The new form factors and real as well as virtual final state radiation have been implemented in the Monte Carlo generator PHOKHARA.

Acknowledgments

Henryk Czyż is grateful for the support and the kind hospitality of the Institut für Theoretische Teilchenphysik of the Karlsruhe Institute of Technology.

[1] I. Estermann, R. Frisch, and O. Stern, Nature **132**, 169 (1932).
[2] M. Rosenbluth, Phys.Rev. **79**, 615 (1950).
[3] R. Mcallister and R. Hofstadter, Phys.Rev. **102**, 851 (1956).
[4] R. Hofstadter, Rev.Mod.Phys. **28**, 214 (1956).
[5] A. Akhiezer and M. Rekalo, Sov.Phys.Dokl. **13**, 572 (1968).
[6] J. Arrington, Phys.Rev. **C68**, 034325 (2003), nucl-ex/0305009.
[7] C. E. Carlson and M. Vanderhaeghen, Ann.Rev.Nucl.Part.Sci. **57**, 171 (2007), hep-ph/0701272.
[8] R. Milner et al. (OLYMPUS), Nucl.Instrum.Meth. **A741**, 1 (2014), 1312.1730.
[9] G. P. Lepage and S. J. Brodsky, Phys.Rev. **D22**, 2157 (1980).
[10] C. Perdrisat, V. Punjabi, and M. Vanderhaeghen, Prog.Part.Nucl.Phys. **59**, 694 (2007), hep-ph/0612014.
[11] A. Denig and G. Salme, Prog.Part.Nucl.Phys. **68**, 113 (2013), 1210.4689.
[12] J. Lees et al. (BaBar Collaboration), Phys.Rev. **D87**, 092005 (2013), 1302.0055.
[13] H. Czyz, A. Grzelinska, and J. H. Kuhn, Phys.Rev. **D81**, 094014 (2010), 1002.0279.
[14] H. Czyz, J. H. Kuhn, E. Nowak, and G. Rodrigo, Eur.Phys.J. **C35**, 527 (2004), hep-ph/0403062.
[15] F. Iachello, A. Jackson, and A. Lande, Phys.Lett. **B43**, 191 (1973).

[16] G. Bardin, G. Burgun, R. Calabrese, G. Capon, R. Carlin, et al., Nucl.Phys. **B411**, 3 (1994).

[17] G. Bardin, G. Burgun, R. Calabrese, G. Capon, R. Carlin, et al., Phys.Lett. **B255**, 149 (1991).

[18] G. Bardin, G. Burgun, R. Calabrese, G. Capon, R. Carlin, et al., Phys.Lett. **B257**, 514 (1991).

[19] T. Armstrong et al. (E760 Collaboration), Phys.Rev.Lett. **70**, 1212 (1993).

[20] M. Ambrogiani et al. (E835 Collaboration), Phys.Rev. **D60**, 032002 (1999).

[21] M. Andreotti, S. Bagnasco, W. Baldini, D. Bettoni, G. Borreani, et al., Phys.Lett. **B559**, 20 (2003).

[22] D. Bisello, S. Limentani, M. Nigro, L. Pescara, M. Posocco, et al., Nucl.Phys. **B224**, 379 (1983).

[23] D. Bisello et al. (DM2 Collaboration), Z.Phys. **C48**, 23 (1990).

[24] M. Ablikim et al. (BES Collaboration), Phys.Lett. **B630**, 14 (2005), hep-ex/0506059.

[25] T. Pedlar et al. (CLEO Collaboration), Phys.Rev.Lett. **95**, 261803 (2005), hep-ex/0510005.

[26] A. Antonelli, R. Baldini, P. Benasi, M. Bertani, M. Biagini, et al., Nucl.Phys. **B517**, 3 (1998).

[27] B. Delcourt, I. Derado, J. Bertrand, D. Bisello, J. Bizot, et al., Phys.Lett. **B86**, 395 (1979).

[28] V. Punjabi, C. Perdrisat, K. Aniol, F. Baker, J. Berthot, et al., Phys.Rev. **C71**, 055202 (2005), nucl-ex/0501018.

[29] O. Gayou et al. (Jefferson Lab Hall A Collaboration), Phys.Rev.Lett. **88**, 092301 (2002), nucl-ex/0111010.

[30] O. Gayou, K. Wijesooriya, A. Afanasev, M. Amarian, K. Aniol, et al., Phys.Rev. **C64**, 038202 (2001).

[31] A. Puckett, E. Brash, M. Jones, W. Luo, M. Meziane, et al., Phys.Rev.Lett. **104**, 242301 (2010), 1005.3419.

[32] T. Pospischil et al. (A1 Collaboration), Eur.Phys.J. **A12**, 125 (2001).

[33] R. Madey et al. (E93-038 Collaboration), Phys.Rev.Lett. **91**, 122002 (2003), nucl-ex/0308007.

[34] E. Geis et al. (BLAST Collaboration), Phys.Rev.Lett. **101**, 042501 (2008), 0803.3827.

[35] L. Andivahis, P. E. Bosted, A. Lung, L. Stuart, J. Alster, et al., Phys.Rev. **D50**, 5491 (1994).

[36] J. Beringer et al. (Particle Data Group), Phys.Rev. **D86**, 010001 (2012).

[37] M. Castellano, G. Di Giugno, J. Humphrey, E. Sassi Palmieri, G. Troise, et al., Nuovo Cim. **A14**, 1 (1973).

[38] H. Czyz, A. Grzelinska, J. H. Kuhn, and G. Rodrigo, Eur.Phys.J. **C33**, 333 (2004), hep-ph/0308312.

[39] H. Czyz, A. Grzelinska, J. H. Kuhn, and G. Rodrigo, Eur.Phys.J. **C39**, 411 (2005), hep-ph/0404078.

[40] S. Binner, J. H. Kuhn, and K. Melnikov, Phys.Lett. **B459**, 279 (1999), hep-ph/9902399.

[41] H. Czyz, A. Grzelinska, and J. H. Kuhn, Phys.Lett. **B611**, 116 (2005), hep-ph/0412239.

[42] H. Czyz, M. Gunia, and J. Kuhn, JHEP **1308**, 110 (2013), 1306.1985.